Ligand-lipid and ligand-core affinity control the interaction of gold nanoparticles with artificial lipid bilayers and cell membranes

Janine Broda, Dr. rer. nat.[a,1], Julia Setzler, Dr. rer. nat.[b,1], Annika Leifert, Dr. rer. nat.[a],
Julia Steitz, Dr. rer. nat.[e], Roland Benz, Dr. rer. nat.[c,d], Ulrich Simon, Dr. rer. nat.[a],
Wolfgang Wenzel, PhD[b,*]

[a]Institute of Inorganic Chemistry, RWTH Aachen University, Aachen, Germany
[b]Institute of Nanotechnology, Karlsruhe Institute of Technology, Karlsruhe, Germany
[c]Rudolf Virchow Center, University of Würzburg, Würzburg, Germany
[d]Department of Life Sciences and Chemistry, Jacobs University Bremen, Bremen, Germany
[e]Institute for Laboratory Animal Science, Medical Faculty, RWTH Aachen University, Aachen, Germany

Abstract

Interactions between nanoparticles (NPs) and biomembranes depend on the physicochemical properties of the NPs, such as size and surface charge. Here we report on the size dependent interaction of gold nanoparticles (AuNPs), stabilized with ligands differing in charge, i.e. sodium 3 (diphenylphosphino)benzene sulfonate (TPPMS) and sodium 3,3′,3″ triphenylphosphine sulfonate (TPPTS), respectively, with artificial membranes (black lipid membranes; BLMs) and HeLa cells. The TPPTS stabilized AuNPs affect BLMs at lower size than TPPMS stabilized ones. On HeLa cells we found decreasing cytotoxicity with increasing particle size, however, with an overall lower cytotoxicity for TPPTS stabilized AuNPs. We attribute size dependent BLM properties as well as reduced cytotoxicity of TPPTS stabilized AuNPs to weaker shielding of the AuNP core when stabilized with TPPTS. We hypothesize that the partially unshielded hydrophobic gold core can embed into the hydrophobic membrane interior. Thereby we demonstrate that ligand dependent cytotoxicity of NP can occur even when the NPs are not translocated through the membrane.

From the Clinical Editor: The use of nanoparticles (NPs) in the clinical setting means that there will be interactions between NPs and cell membranes. The authors investigated the underlying processes concerning cellular uptake and potential toxicity of gold nanoparticles (AuNPs) using particles with ligands different sizes and charges. The findings should further enhance existing knowledge on future design of safer NPs in the clinic.

Key words: Gold nanoparticles; Colloidal synthesis; Artificial black lipid membranes; Electrophysiology; Nanotoxicity; Size and surface charge effect

The use of nanoparticles (NPs) in technology and medicine is rapidly increasing and accompanied by a large number of studies investigating the interactions between NPs and human cells.[1-8] Biocompatibility, toxicity and the ability to penetrate cells are three critical factors that will determine the utility of NPs in e.g. clinical applications. Among the different types of nanomaterials studied, gold nanoparticles (AuNPs) have found wide interest because of their stability, size controlled synthesis and their versatile surface chemistry. However, the long term health effects associated with the internalization of AuNPs are a matter of concern. Therefore, it is of great importance to understand the complex processes that control the cellular uptake and intracellular fate of AuNPs.

The interaction between the cell membrane and AuNPs is of particular interest, as the cell membrane is the basic structure of the cell that may be breached with concomitant cytotoxicity. Several studies demonstrated that NPs can strongly interact with cell membranes, either in adsorbing onto them or by affecting the membrane integrity, leading to the formation of holes. The morphology of the resulting pore depends on the NP size and surface charge.[9-11] Ginzburg *et al* presented a mesoscale thermodynamic model describing the transitions in membrane

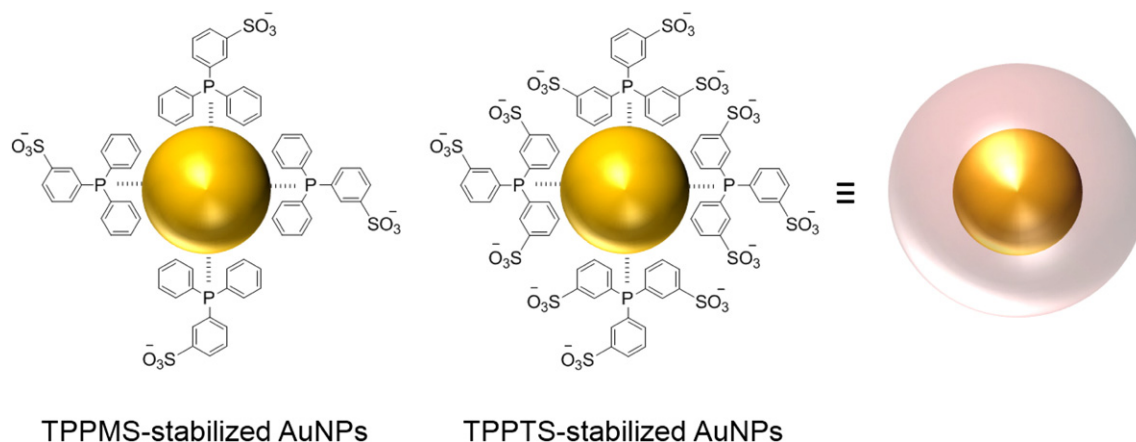**TPPMS-stabilized AuNPs**   **TPPTS-stabilized AuNPs**

Figure 1. Schematic illustration of either sodium 3-(diphenylphosphino)benzene sulfonate (TPPMS) stabilized AuNPs (left), sodium 3,3′,3″-triphenylphosphine sulfonate (TPPTS) stabilized AuNPs (middle), and the simplified representation of AuNPs with their surrounding ligand shell, depicted in red (right). The particles as well as their surrounding ligands are not drawn to scale.

morphology observed after exposure of the membrane to various types of NPs in the size range of 1 10 nm.[12] The simulations demonstrate that the NP membrane interactions are both size and charge dependent. Hydrophobic AuNPs are likely to be absorbed into the membrane whereas strongly charged NPs attract the head groups of the lipid molecules leading to a phospholipid arrangement in the form of a bilayer around the NPs. These theoretical findings for hydrophobic NPs are in accordance with experimental results by Bothun, who reported that small hydrophobic 5.7 nm sized decanethiol stabilized silver NPs in the proximity of a lipid bilayer are embedded directly into the lipid bilayer.[13] Similarly findings were reported by Rasch *et al* for hydrophobic AuNPs.[14] The authors studied the interactions of sub 2 nm dodecanethiol stabilized AuNPs with model phosphatidylcholine lipid vesicles. The visualization of the vesicles *via* cryoTEM showed that the vesicle membranes were completely loaded with a dense monolayer of AuNPs without disrupting the structure of the bilayer. Thus, two requirements must be fulfilled to facilitate the embedding of NPs into the hydrophobic membrane interior. Firstly, the NPs must be small enough (<8 nm) to fit into the hydrophobic bilayer area and, secondly, they must exhibit a hydrophobic surface.[15]

Biological activity of NPs is widely determined by nanomaterial properties such as size, shape, and surface chemistry.[16,17] Extensive studies have focused on the influence of surface effects of AuNPs interacting with biological systems.[4,6,7,18-20] The stabilizing ligands of AuNPs can promote binding affinity, potentially resulting in either endocytosis or direct penetration of the surface membrane.[21] Nonspecific attractive forces that promote cellular contact and particle uptake can be dictated by the surface charge, which controls the NP interactions with charged phospholipid head groups or protein domains on cell surfaces.[22] Generally, cationic surface units exert stronger effects to the cell surface than their anionic counterparts.[18,23,24] Nevertheless, there has been evidence of uptake of negatively charged particles despite the unfavorable interaction between the particles and the negatively charged cell membrane.[25]

In addition to the surface charge dependence, a size dependence of AuNP internalization and cytotoxicity was

shown.[1,2,26] This can be related to a higher surface area to volume ratio as well as the easier access to intracellular sites, such as the cell nucleus, due to the small size, which hardly exceeds those of complex small molecules. In previous studies we have demonstrated a size dependent cytotoxicity of 0.8, 1.2, 1.4, 1.8 and 15 nm sized sodium 3 (diphenylphosphino)benzene sulfonate (TPPMS) stabilized AuNPs.[26] The highest toxic effect was observed for AuNPs with a diameter of 1.4 nm (Au1.4MS). It was discovered that these particles cause oxidative stress finally leading to cell death *via* a necrotic pathway.[27] The high cytotoxicity of Au1.4MS is attributed to the weak binding of the phosphine ligands to the particle surface as the incubation of Au1.4MS with strong binding thiol ligands led to a reduced cytotoxicity.[27] Thus, it is assumed that the loss of the phosphine ligands during interactions with cells leads to the formation of an unshielded catalytically active AuNP surface[28] which may be the cause of the high cytotoxicity.

However, uptake experiments give only cell level evidence of membrane disruption by AuNPs. Understanding of molecule level details, e.g. disturbances on cell membranes are still lacking due to the limitations of current experimental techniques. In this context lipid bilayer experiments provide an effective approach to combine experimental studies and modeling to characterize the interaction of NP with membranes.

Artificial bilayers comprised of phospholipids with zwitter ionic head groups, which are the most common components of cell membranes and the optimal lipid substitute for simple model cell membranes[29], can be easily prepared in solution either as three dimensional vesicles[14,18] or as two dimensional supported[30] or free standing structures.[31] Black lipid bilayer membranes (BLM) are free floating membranes which are formed between two compartments with a defined composition. They are ideally suited for the investigation of AuNP membrane interactions without any potential disturbance through a supporting substrate.[32]

Here, we present a thorough investigation of the complex interaction patterns of AuNPs with diameters ranging from 1.4 15 nm stabilized with either TPPMS (Figure 1 left) or sodium 3,3′,3″ triphenylphosphine sulfonate (TPPTS, Figure 1

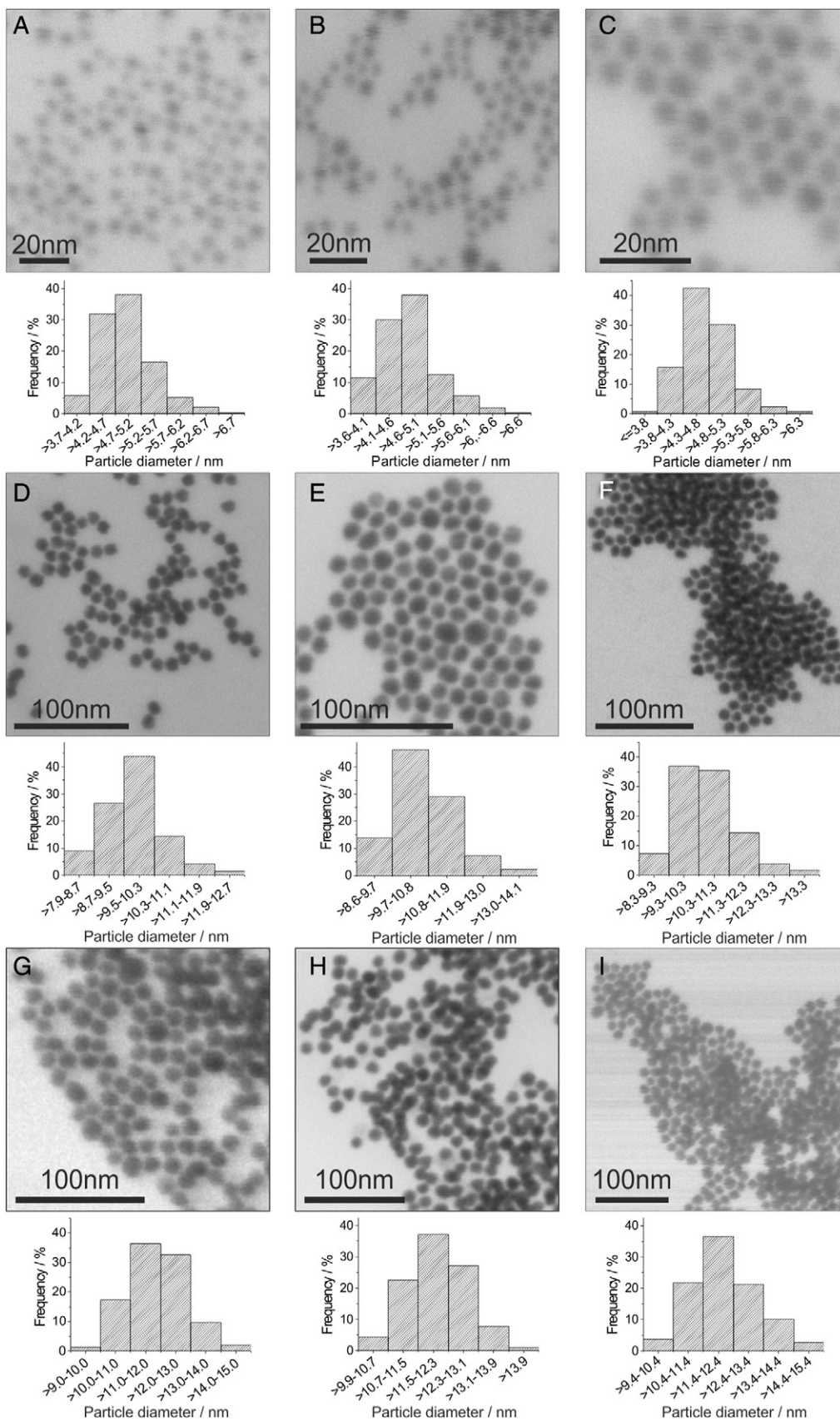Figure 2. SEM-T images and corresponding histograms of Au4.7Citrate **(A)**, Au4.7MS **(B)**. Au4.7TS **(C)**, Au9.8Citrate **(D)**, Au10.7MS **(E)**, Au10.5TS **(F)**, Au11.9Citrate **(G)**, Au12.0MS **(H)** and Au12.3TS **(I)** particles, respectively.

Table 1
Summary of the analytical data for all synthesized AuNPs. The UV/Vis and DLS data are recorded on colloidal aqueous solutions.

Size AuNPs	Ligand	λ_{max}/nm	d_h/nm	PdI	d (SEM-T)/nm
1.4 nm	**TPPMS**	/	/	/	1.4 ± 0.1
	Citrate	514	10.0	0.33	4.7 ± 0.5
~ 5 nm	**TPPMS**	519	10.1	0.39	4.7 ± 0.5
	TPPTS	521	10.3	0.25	4.7 ± 0.5
	Citrate	519	16.0	0.15	9.8 ± 0.8
~ 10 nm	**TPPMS**	522	17.0	0.16	10.7 ± 1.1
	TPPTS	522	17.2	0.12	10.5 ± 1.0
	Citrate	518	19.7	0.17	11.9 ± 1.0
~ 12 nm	**TPPMS**	522	19.3	0.16	12.0 ± 0.8
	TPPTS	522	18.9	0.19	12.3 ± 1.0
	Citrate	521	21.2	0.21	14.6 ± 1.5
~ 15 nm	**TPPMS**	524	21.9	0.13	14.2 ± 1.4
	TPPTS	524	21.5	0.13	15.3 ± 1.7

middle) with artificial membranes and cells. In contrast to other studies which either compare hydrophobic with hydrophilic surface modifications or cationic with anionic surface charges, we investigated the influence of differently sized AuNPs stabilized with ligands which exhibit either one or three negative ligand charges. We measured the membrane conductance of zwitterionic BLMs exhibited by the phospholipid bilayer upon AuNP interaction. Based on these results we formulate a hypothesis that helps understanding how the chemical moieties of the stabilizing ligands in addition to the AuNP size impact their interaction with membranes. Finally, we compare these results to *in vitro* studies using the XTT cytotoxicity assays.

Methods

Syntheses

AuTPPCl was synthesized by using the protocol of Reed et al[33] (details for all NP see supplemental information). Triphenylphosphine 3 monosulfonic acid (TPPMS) was prepared according to Ahrland et al.[34] Au1.4TPP was synthesized by a method of Schmid et al.[35] For synthesis of 5 nm sized colloidal AuNPs HAuCl$_4$ was reduced with NaBH$_4$ in adaption to Selvakannan et al.[36] Synthesis of about 10 nm sized colloidal AuNPs was performed by a citrate reduction of HAuCl$_4$ according to Olmedo et al.[37] For synthesis of about 12 nm AuNP the Turkevich Method was used.[38] (for details and chemicals see SI).

Artificial membrane experiments

Black lipid membrane experiments[1] were performed using a small Teflon chamber with two compartments (named as *cis* side and *trans* side) connected by a small hole with 0.5 mm^2 surface area (details see SI). For the membrane potential V_a we applied up to 150 mV through silver/silver chloride electrodes inserted into the aqueous salt solutions on both sides of the membrane. The membrane current I was measured on a strip chart recorder, using a current to voltage converter made with a Burr Brown

operational amplifier. All experiments were repeated several times. AuNPs were always added to the *cis* side of the membrane.

Cytotoxicity assay

HeLa mouse cervix carcinoma cells were cultured in tissues culture plates (*Becton Dickinson*) in low glucose Dulbecco's modified Eagle's medium (DMEM, *Gibco*) (details see SI). Confluent cells were harvested with the help of trypsin EDTA and plated in 96 well tissues culture plates at initial densities of 2000 cells/well and treated as described in the SI. Cell growth was tested by the colorimetric XTT assay. The supernatant was removed and cells were washed 2 3 times with 200 µL/well of sterile phosphate buffered saline (PBS, *Sigma Aldrich*). 80 µL/well of fresh DMEM and 20 µL/well of XTT (*Sigma Aldrich*) solution were added and incubated for 2 3 h until color change was detected. Plates were measured with an ELISA reader (*Mulitiskan, Thermo Scientific*) at 450 nm with a reference wavelength of 690 nm. Cell survival was plotted against the applied gold concentrations with *Origin* and analyzed with the sigmoidal dose response fit to determine the IC$_{50}$ value. The given standard deviations represent the error of the dose response fit and not the error of the measurements.

Results

Nanoparticle syntheses and characterization

Different routes were followed to synthesize TPPMS or TPPTS stabilized (Figure 1) AuNPs with varying sizes. The TPPMS stabilized AuNPs with diameters of 1.4 nm and 15 nm were used in several earlier studies where the syntheses and the analytical data are described.[26,27,39] To investigate the interactions of AuNPs in the size range of 5 12 nm, new TPPMS as well as TPPTS stabilized AuNPs were synthesized (see Methods and SI). Characterization with dynamic light scattering (DLS) depicts that for all particle species some aggregates are present in the colloidal solution. The TPPMS and TPPTS stabilized particles show the same hydrodynamic diameter d_h as the citrate capped ones (Figure SI 1). By SEM T images the mean particle diameters for all three particle species was determined to be (4.7 ± 0.5) nm (Figure 2, A C).

Citrate capped AuNPs with sizes of about 10 nm and 12 nm were synthesized following Olmedo et al[37] and Turkevich et al,[38] respectively. Briefly, a chloroauric acid solution was refluxed and a citrate solution was added. The citrate serves as stabilizing ligand as well as reducing agent. By varying the citrate to chloroauric acid concentration ratio the size of the AuNPs can be adjusted. The AuNPs which were synthesized according to Olmedo et al[37] show a mean particle diameter of (9.8 ± 0.8) nm (Figure 2, D). The UV/Vis spectrum depicts an absorbance maximum of 519 nm. Ligand exchange reactions with either TPPMS or TPPTS led to a shift of the absorbance maximum to 522 nm (Figure SI 2). In addition, the plasmon resonance peak is not as broad as for citrate stabilized ones. DLS measurements show that no aggregates are present in the colloidal solution. The hydrodynamic diameter increases slightly after the ligand exchange (Figure SI 2). The particle diameters
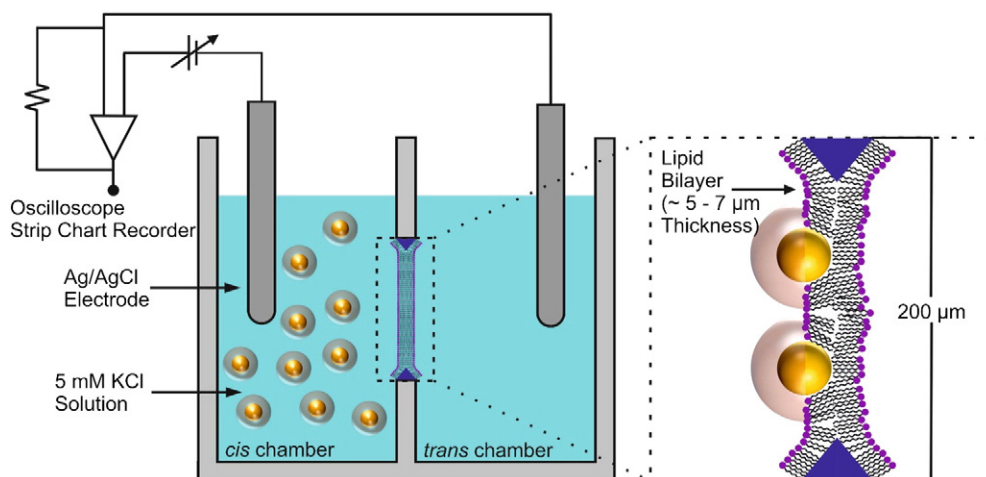
Figure 3. Schematic setup of the electrophysiological BLM experiments. Two compartments (*cis* and *trans*) are filled with KCl solutions which serve as electrolyte and separated by a small aperture onto which the lipid bilayer membrane is formed. Two electrodes enable the application of an external potential to the membrane and the conductivity was detected with either an oscilloscope or a flip chart recorder. AuNPs are added to the *cis* compartment and the interactions of the particles with the membrane are monitored. The simplified scheme displays the insertion of individual unshielded hydrophobic gold cores into the membrane. Please note that the bilayer thickness, the particle diameter as well as their surrounding ligand shell are not drawn to scale with respect to the aperture. The layout of the scheme is for a better comparability based on the figure used in the work of Carney *et al.*[31]

were determined to be (10.7 ± 1.1) nm and to (10.5 ± 1.0) nm (Figure 2, E and F) for TPPMS and TPPTS stabilized AuNPs, respectively. This slight increase in particle diameter is in accordance with the increased hydrodynamic diameter derived from DLS measurements.

The UV/Vis spectrum of the citrate capped particles synthe sized according to Turkevich *et al*[38] exhibits an absorbance maximum of 519 nm. Ligand exchange reactions with either TPPMS or TPPTS led to a shift of the absorbance maximum to 522 nm. DLS measurements confirmed that no aggregates are present in the colloidal solution and that the hydrodynamic diameter does not show significant changes after the ligand exchange (Figure SI 3). The mean particle diameters were determined to be (11.9 ± 0.9) nm for citrate capped ones (Figure 2, G) and (12.0 ± 0.8) nm and (12.3 ± 1.0) nm for TPPMS and TPPTS stabilized ones, respectively (Figure 2, H and I).

The analytical data for all particles which were investigated in artificial lipid bilayer experiments and in cell tests are summarized in Table 1.

Lipid bilayer conductance

In order to investigate the size and surface charge dependent interactions between AuNPs and cell membranes, we performed experiments on artificial zwitterionic diphytanoyl phosphatidyl choline (DiphPC) lipid bilayer membranes (methods see SI). This system is a widely used model for a cell membrane because it simultaneously permits access to the solution and electrical control of both sides of the bilayer, allowing the mimicking of physiological conditions. A schematic setup of the black lipid membrane (BLM) experiment[40] is shown in Figure 3. Two compartments (*cis* and *trans*) are separated by a small aperture onto which the lipid bilayer membrane is formed. The

compartments are each filled with KCl as electrolytic solution. External membrane potentials are applied using Ag/AgCl electrodes, and the membrane conductivity is amplified using an oscilloscope or a strip chart recorder.

Before the conductance measurements of the membranes bathed in the AuNP solutions were performed, reference measurements were carried out in order to verify that the lipid bilayer is stable and to exclude multilayer formation. When the lipid membrane was proven to be defect free, AuNP solutions were added to one compartment of the BLM setup to obtain an end concentration of 0.5 mM referring to gold was established. A time dependent membrane potential ranging from 0 180 mV was applied and the membrane current was recorded up to 15 minutes.

First, the size dependent interactions of differently sized TPPMS stabilized AuNPs, namely Au1.4MS, Au4.7MS, Au10.7MS, Au12MS and Au15MS, were determined. Repre sentative strip chart records for the current measurements of the lipid bilayer alone and the differently sized TPPMS stabilized AuNPs are shown in Figure 4. The reference measurement (A) shows that no change in current is observed when the bilayer is intact. In the case of Au1.4MS the applied voltage was changed from 0 mV to 100 mV and back to 0 mV. The voltage change can be seen in the two sharp peaks in B but no increase in current was observed indicating that the particles do not lead to a membrane disturbance. Au4.7MS and Au10.7MS did not lead to an increase in current, too (C and D). However, Au12MS and Au15MS affect the bilayer and lead to a change in the measured current as can be seen in E and F, respectively. Thus, larger sized TPPMS stabilized AuNPs interact with the membrane leading to a change of conductance.

In addition to the size dependent interactions of AuNPs with lipid membranes, the ligand dependent interactions were exam ined. Representative strip chart recordings for conductivity
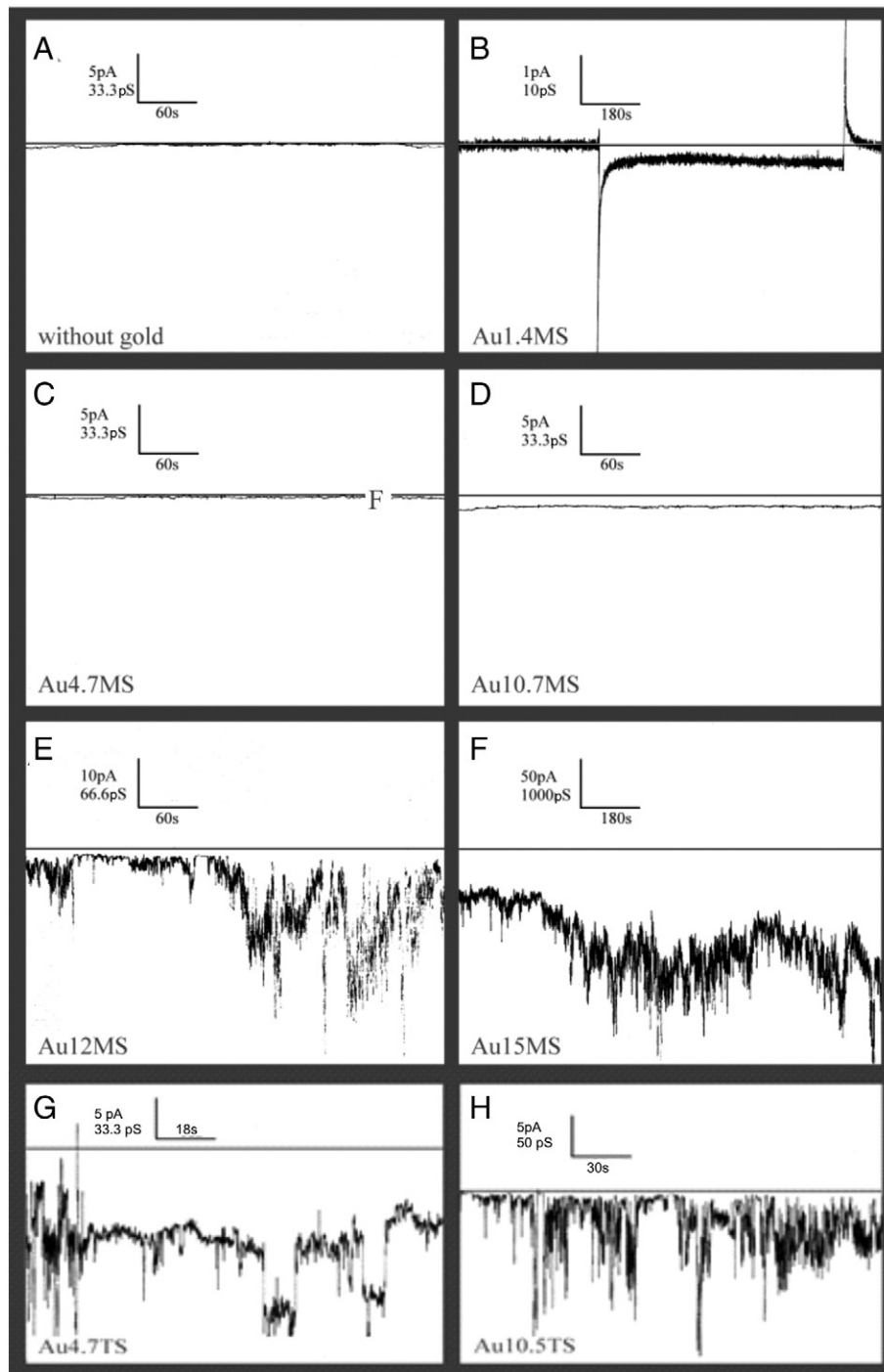
Figure 4. Representative current measurements of different sized TPPMS-stabilized AuNPs: **(A)** reference measurement without AuNPs, applied voltage −150 mV **(B)**, Au1.4MS, applied voltage 0 mV, −100 mV, 0 mV **(C)**, Au4.7MS, applied voltage −150 mV **(D)**, Au10.7MS, applied voltage −150 mV **(E)**, Au12MS, applied voltage −150 mV **(F)** Au15MS, applied voltage −50 mV. Representative current measurements of different sized TPPTS-stabilized AuNPs: **(G)** Au4.7TS, applied voltage −150 mV, **(H)** Au10.5TS, applied voltage −100 mV. The scale (membrane current, membrane conductance and time) is added to each panel. The observation time depends on the stability of the membrane in the experiment. Small AuNPs **(A-F)** show no effect on the membrane, whereas AuNPs with a size larger than 12 nm lead to an increase of conductance. For TPPTS-AuNPs both AuNPs **(G and H)** lead to an increase of membrane conductance.

measurements of Au4.7TS and Au10.5TS are shown in Figure 4. In contrast to TPPMS stabilized AuNPs, Au4.7TS and Au10.5TS already affect the lipid bilayer, leading to an increased

conductivity. As the 4.7 and 10.5 nm sized AuNPs already led to disturbances in the lipid membrane, larger sized particles were not measured.
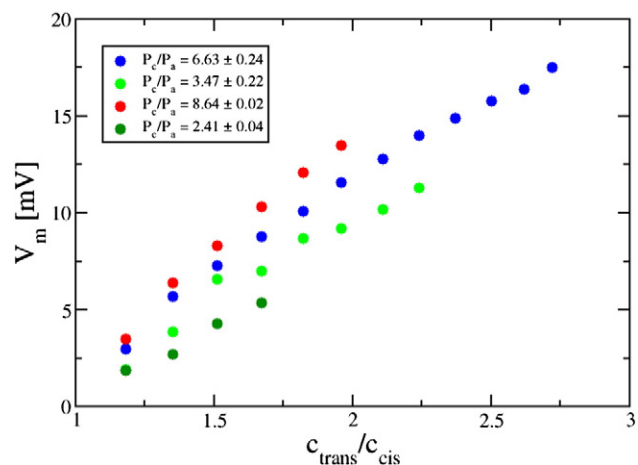
Figure 5. Results of four independent ion selectivity measurements for Au15MS (every independent experiment is depicted in a different color). The cation/anion permeability ratio (P_c/P_a) is in all measurements higher than one indicating that the membrane is preferentially selective for cations. The average and variance of (P_c/P_a) are shown in the legend.

Furthermore, we performed selectivity measurements for Au15MS to investigate whether cations or anions are responsible for the measured increased membrane conductance (see Figure 5).

The magnitude of conductance through the membrane is a measure of the membrane disturbance. To gain information about the degree of disturbances the measured conductivities of AuNP incubated bilayers are compared to conductance observed for Gramicidin A (GramA) incubated lipid bilayers. GramA is a polypeptide antibiotic which induces pore formation in the membrane. For Gram A we observed an about 1000 fold increase of the current flow as compared to all tested AuNPs (see Figure SI 4). This suggested that AuNPs did not lead to pore formation but to structural disturbances generated in the membrane upon AuNP membrane interactions. Since the transfer of charged groups to the hydrophobic membrane interior is energetically unfavorable and the particles are partly not small enough to fit the width of the bilayer (~8 nm),[15] we hypothesize that the ligands may be displaced, at least partially, when AuNPs enter the membrane, leaving an essentially hydrophobic gold core[41] in direct contact with the hydrophobic center of the membrane. The embedding of the gold core into the membrane interior can lead to structural disturbances of the membrane structure also leading to a higher dielectric constant of the membrane interior resulting in a higher permeability for cations which is measured as current flow. This hypothesis is also helpful in the interpretation of the selectivity measurements as the unshielded gold core is positively polarized, facilitating the transport of cations from the solution in agreement with the experimental observations.

The displacement of phosphine ligands attached to AuNPs was already demonstrated for Au1.4TPP by a dissociation equilibrium of bound and free ligand molecules in solution via ^{31}P NMR spectroscopy.[42] Furthermore, the modeling of Au1.4MS in contact with the hERG potassium ion channel suggests that the gold core is embedded in the entrance of the ion channel after the partial or complete loss of the TPPMS ligand shell.[43]

The embedding of a partially unshielded hydrophobic gold core into the membrane interior is in agreement with modeling results of Ginzburg et al[12] who described the incorporation of hydrophobic AuNPs into the membrane. Vesicle studies conducted by Van Lehn et al[44] showed that partially hydrophobic stabilized AuNPs fuse into the cell membrane driven by the hydrophobic effect which is even more favorable when the ligands are able to fluctuate easily. The spontaneous fusion of AuNPs with lipid bilayers was also observed by Carney et al.[31] In contrast to the experiments performed in this work, Carney et al measured the capacitance instead of the conductivity. It was shown that AuNPs in a size range of 4 6.5 nm stabilized with a mixture of hydrophilic and hydrophobic ligands are incorporated into the membrane interior. AuNPs with sizes of 7.2 nm as well as AuNPs stabilized with hydrophilic ligands were not incorporated into the membrane. This is in good agreement with the results observed in this work as we assume that the hydrophobic unshielded gold core is partially incorporated into the membrane and not the AuNPs including their hydrophobic ligand shell.

Cyanide degradation experiments

Nevertheless, the hypothesis that the gold core in direct contact with the membrane leads to the measured current flow does not explain the size dependent differences in the conductivity measurements for the differently stabilized AuNPs. Thus, the accessibility of the gold core for the TPPMS and TPPTS stabilized particles was considered. TPPMS exhibits only one negative charge wherefore a high packing density is assumed. By contrast, TPPTS exhibits three negative charges which cause higher repulsive forces between the ligands eventually resulting in a reduced packing density. To confirm this assumption the stability of both TPPMS and TPPTS stabilized AuNPs was studied by probing the ligands' ability to shield the inorganic core against strongly etching cyanide anions (CN).[45,46] Since a high ligand density leads to a high steric shielding of the AuNPs and thus hinders the diffusion of CN to the particle surface, the digestion of the particles can be related to the number of ligands on the AuNP surface.[47]

Because AuNPs with sizes of 4.7 and 10.7 nm showed ligand dependent behavior in the BLM measurements, particles with similar sizes were utilized for the CN etching experiments. The corresponding plasmon resonance absorbance maximum of the colloidal solutions was adjusted to an optical absorbance with a good signal to noise ratio and either 0.5 M or 2.5 M KCN solutions were added. The concentration of the KCN solution was higher for larger AuNPs to compensate the greater total number of gold atoms per NP. The decomposition rate of the AuNPs was monitored by time dependent UV/Vis spectroscopy. The stability of the particles is observed by temporal changes in the absorbance spectra, namely a decrease of the intensity at the surface plasmon resonance maximum accompanied by a possible increase of the absorbance at higher wavelength. The latter is caused by the electromagnetic coupling of AuNPs upon aggregation. Furthermore the appearance of new signals at 204, 211, 228 and 238 nm, respectively, indicates the formation of [Au(CN)$_2$] complexes.[48] The associated decrease of the
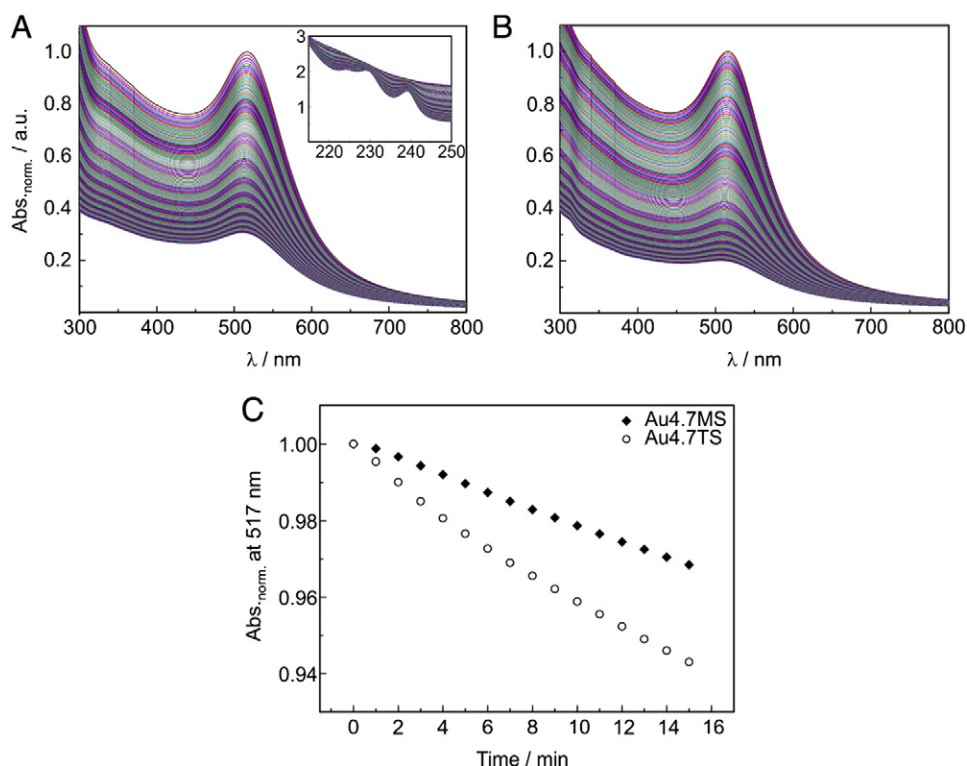
Figure 6. Normalized UV/Vis-spectra of the decomposition of AuNPs by the addition of 0.5 M KCN-solution for **(A)** Au4.7MS with the formation of $[Au(CN)_2]$ complexes shown in the inset and **(B)** Au4.7TS. The spectra were monitored every 5 minutes over a period of 20 h. **(C)** Decrease of the surface plasmon resonance absorbance at 517 nm plotted against the time. The spectra were monitored every minute over a period of 15 minutes.

surface plasmon resonance was analyzed by plotting it as a function of time. Due to the time frame used in the BLM measurements only the first 15 minutes was analyzed.

Figure 6 shows the UV/Vis spectra of the AuNP decompo sition by addition of KCN for Au4.7MS (a) and Au4.7TS (b) as well as the absorbance decay in the first 15 minutes (c). The appearance of the $[Au(CN)_2]$ complexes is shown in the inset of the UV/Vis spectra for Au4.7MS. By the addition of KCN to both Au4.7MS and Au4.7TS the surface plasmon resonance absorbance decays in a steady way. The decrease for Au4.7TS is faster compared to Au4.7MS indicating a better shielding of the Au core in Au4.7MS. To quantify the rate of decomposition the time dependent decrease of the plasmon resonance absorbance can be fitted by either a first or a second order exponential decay function.[46,49] Nevertheless, it was not possible to fit our decay curves with an exponential decay function so that the data can just be seen as semi quantitative.

Figure 7 shows the corresponding diagrams for about 10 nm sized AuNPs with the appearance of the $[Au(CN)_2]$ complexes shown in the inset of the UV/Vis spectra for Au10.3MS. For larger sized AuNPs the plasmon resonance absorbance of Au10.3MS decreases steadily over time whereas the absorbance of Au9.7TS decreases at the beginning of the reaction and then shifts toward higher wavenumbers, which we attribute to the formation of AuNP aggregates. After this aggregation formation a slower decay rate of Au9.7TS compared to Au10.3MS is observed. This can be explained by a kinetic

hindrance of the decomposition reaction in larger aggregates compared to single particles.

The comparison of the decomposition of smaller and larger particles indicates that AuNP digestion with CN depends not only on the stabilizing ligand but also on the NP size. This could be explained as follows: during the decomposition of the AuNPs with CN smaller particles and fragments are formed. Small sized AuNPs exhibit a high surface area and thus need a large number of stabilizing ligands.[50,51] Due to this high number of stabilizing ligands the fragments occurring during decomposi tion can be shielded appropriately so that the formation of aggregates does not appear. Larger sized AuNPs exhibit a lower surface area and thus a lower number of stabilizing ligands.[50,51] This overall lower amount of stabilizing ligands could lead to the formation of aggregates since the occurring fragments may not be stabilized properly. For Au9.7TS a red shift of the plasmon resonance is observed indicating that aggregation occurs. By contrast, Au10.3MS displays just a slight shift of the plasmon resonance at a late stage of the decomposition reaction. This early appearance of aggregates for Au9.7TS in combination with the faster decay rates for both sized TPPTS stabilized AuNPs indicates a lower number of ligands per particle for these particles compared to TPPMS stabilized AuNPs.

Hence, with the use of strongly etching CN it was shown that TPPMS stabilized AuNPs exhibit a better ability to shield the inorganic core indicating a higher ligand density. These results support the hypothesis that a displacement of the ligands
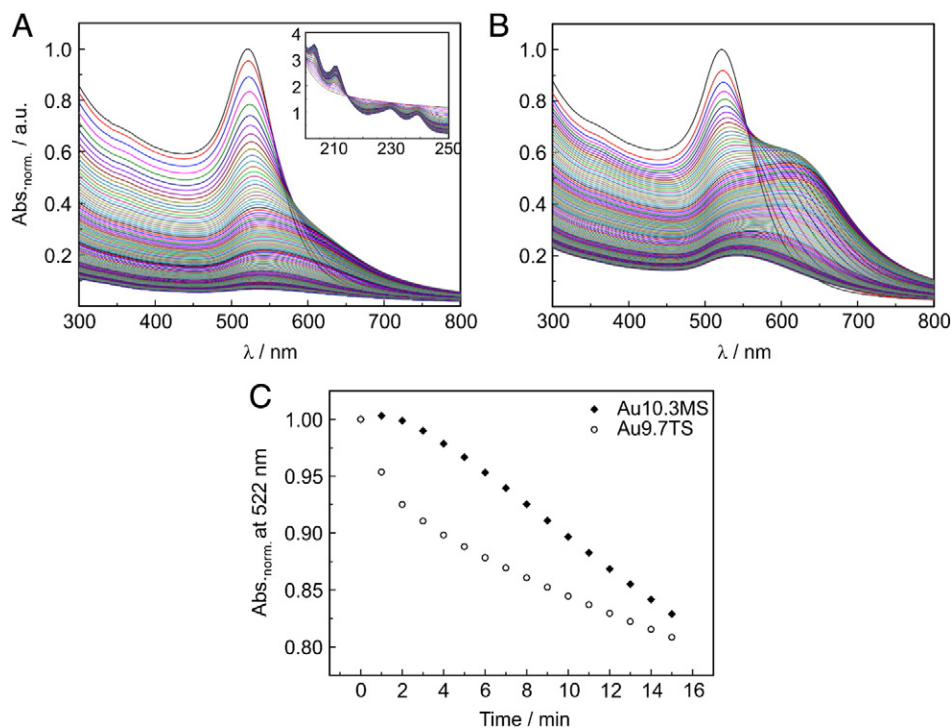
Figure 7. Normalized UV/Vis-spectra of the decomposition of AuNPs by the addition of 2.5 M KCN solution for **(A)** Au10.3MS with the formation of $[Au(CN)_2]^-$ complexes shown in the inset and **(B)** Au9.7TS. The spectra were monitored every 5 minutes over a period of 20 h. **(C)** Decrease of the surface plasmon resonance absorbance at 522 nm plotted against the time. The spectra were monitored every minute over a period of 15 minutes.

leads to an interaction of the gold core with the lipid membrane. With these findings it can be further explained that TPPTS stabilized AuNPs interact already at smaller particle sizes with the membrane due to their lower stability.

Discussion

In order to compare the results obtained on lipid bilayer membranes with actual cell membranes, we have tested the above described AuNPs regarding their cytotoxicity toward HeLa cervix carcinoma epithelial cells (see SI for methods). In an earlier study we have shown for TPPMS stabilized particles that Au1.4MS is the most cytotoxic species. Smaller particles as well as 15 nm sized TPPMS stabilized particles were found to be less toxic.[26] In this work we analyze whether besides the particle size the surface charge of the stabilizing ligands has an influence on the cytotoxicity. Therefore we used the XTT (2,3 bis (2 methoxy 4 nitro 5 sulfophenyl) 2*H* tetrazolium 5 carboxanilide) vitality assay by testing the cells during the logarithmic growth phase and determined the respective IC_{50} values (see Figure 8).

Generally, the cytotoxicity decreases with increasing particle size, which is in good agreement with our previous findings.[26] The most toxic species, namely the Au1.4MS shows an IC_{50} value of 43 μM. Au4.7MS shows an IC_{50} value of 580 μM and all larger sized TPPMS stabilized particles have IC_{50} values around 1800 μM. By contrast, Au4.7TS shows an IC_{50} value of 1912 μM whereas all larger sized TPPTS stabilized AuNPs have

IC_{50} values around 5500 μM. However, all TPPTS stabilized AuNPs were found to be less toxic than TPPMS stabilized ones.

Based on the results of the lipid bilayer measurements, where the TPPTS stabilized AuNPs already led to disturbances of the membrane at sizes of 4.7 nm, a higher cytotoxicity of these AuNPs compared to the TPPMS stabilized ones would be expected. These apparently contradictory findings in lipid bilayer membrane test and cytotoxicity test may be explained with a proposed uptake mechanism of different charged AuNPs by Cho *et al.*[20] They hypothesized that the uptake process can generally be described in two steps: the adsorption of AuNPs onto the cell surface followed by an internalization by the cell. In contrast to the used zwitterionic bilayer in the membrane study mammalian cell membranes typically possess an overall negative electric feature. Therefore, the TPPTS stabilized AuNPs with three negative charges per ligand would be highly repelled from the negative cell surface as long as the ligand shell stays intact, preventing them widely from cell adhesion. As discussed before, partial loss of the ligand shell results from dissociation equilibrium of bound and free ligand molecules in solution, which consequently results in a lowering of the total surface charge of the particles. For particle uptake the dissociation equilibrium has to be shifted in favor of lower surface charge and higher hydrophobicity, which can cause slower uptake resulting in an overall lower cytotoxicity for the TPPTS stabilized AuNPs. Another model by Chen *et al*, referred to as film tension model, further supports this assumption as it suggests that hydrophobic particles are more readily internalized than their less hydrophobic counterparts due to the hydrophobicity of the membrane
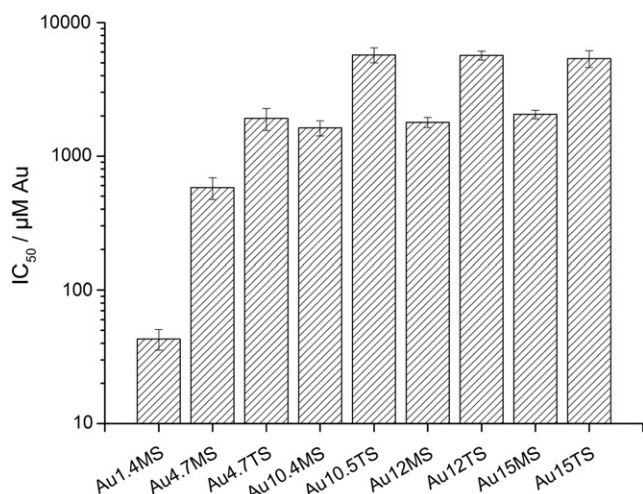
Figure 8. IC_{50} values of different sized TPPMS- and TPPTS-stabilized AuNPs achieved from citrate-stabilized AuNPs. IC_{50} values are drawn in a logarithmic scale in given in μM Au.

interior.[52] For semi hydrophobic NPs, a continuum may exist in which the particles' ability to contact a surface membrane is determined by their relative hydrophilicities.[16] Taking into consideration the lower stability of TPPTS stabilized AuNPs we assume that after a partial loss of stabilizing ligands the resulting hydrophobic gold core could be internalized into the membrane. This would only lead to membrane disturbances but not to membrane distortion as control measurements with Gramicidin S revealed. Thus, this internalization should not result in a cytotoxic behavior. Due to the high surface energy of the unshielded gold core, the stabilization within the hydrophobic membrane interior would energetically be favored so that the AuNPs would be trapped and can no longer contribute to the cytotoxicity. This different behavior in cytotoxicity and cellular damage is consistent with the results by Pernodet et al.[53] They found that even though 13 nm citrate capped AuNPs are non toxic they promote the formation of abnormal actin filaments. Thus, it is important to differentiate between cytotoxicity and cellular damage.

In summary we have observed size dependent differential conductivities of zwitterionic DiphPC membranes upon AuNP interaction. The presence of TPPTS or TPPMS stabilized AuNPs with diameters of approximately 5 nm and 12 nm respectively, induced a membrane current in our experiments. Ion selectivity measurements suggest that the current is carried preferentially by cations. The cytotoxicity of the particles decreases with increasing particle size with an overall lower cytotoxicity for TPPTS stabilized AuNPs. These findings are commensurate with a hypothesis, where the ligands are partially stripped off from the AuNP which inserts an accessible hydrophobic AuNP into the hydrophobic core of the membrane. With cyanide degradation experiments we could show that the size dependent differences in the BLM conductivity measure ments for the differently stabilized AuNPs are due to a better shielding of the AuNP core when stabilized with TPPMS ligands. This illustrates that cytotoxicity of NP is size and ligand dependent and that NP can cause cytotoxic effects, even when the NPs are not translocated through the membrane.

Appendix A. Supplementary data

Supplementary data to this article can be found online at http://dx.doi.org/10.1016/j.nano.2015.12.384.

References

1. Chithrani BD, Chan WCW. Elucidating the mechanism of cellular uptake and removal of protein-coated gold nanoparticles of different sizes and shapes. *Nano Lett* 2007;**7**:1542-50.
2. Chithrani BD, Ghazani AA, Chan WCW. Determining the size and shape dependence of gold nanoparticle uptake into mammalian cells. *Nano Lett* 2006;**6**:662-8.
3. Jiang X-M, Wang L-M, Chen C-Y. Cellular uptake, intracellular trafficking and biological responses of gold nanoparticles. *J Chin Chem Soc* 2011;**58**:273-81.
4. Kim ST, Saha K, Kim C, Rotello VM. The role of surface functionality in determining nanoparticle cytotoxicity. *Acc Chem Res* 2013;**46**: 681-91.
5. Lundqvist M, Stigler J, Elia G, Lynch I, Cedervall T, Dawson KA. Nanoparticle size and surface properties determine the protein corona with possible implications for biological impacts. *Proc Natl Acad Sci* 2008;**105**:14265-70.
6. Rivera-Gil P, Jimenez De Aberasturi D, Wulf V, Pelaz B, Del Pino P, Zhao Y, et al. The challenge to relate the physicochemical properties of colloidal nanoparticles to their cytotoxicity. *Acc Chem Res* 2012;**46**: 743-9.
7. Schaeublin NM, Braydich-Stolle LK, Schrand AM, Miller JM, Hutchison J, Schlager JJ, et al. Surface charge of gold nanoparticles mediates mechanism of toxicity. *Nanoscale* 2011;**3**:410-20.
8. Soenen SJ, Manshian B, Montenegro JM, Amin F, Meermann B, Thiron T, et al. Cytotoxic effects of gold nanoparticles: a multiparametric study. *ACS Nano* 2012;**6**:5767-83.
9. Hong S, Bielinska AU, Mecke A, Keszler B, Beals JL, Shi X, et al. Interaction of poly(amidoamine) dendrimers with supported lipid bilayers and cells: hole formation and the relation to transport. *Bioconjug Chem* 2004;**15**:774-82.
10. Leroueil PR, Hong S, Mecke A, Baker JR, Orr BG, Banaszak Holl MM. Nanoparticle interaction with biological membranes: does nanotechnology present a Janus face? *Acc Chem Res* 2007;**40**:335-42.
11. Mecke A, Majoros IJ, Patri AK, Baker JR, Banaszak Holl MM, Orr BG. Lipid bilayer disruption by polycationic polymers: the roles of size and chemical functional group. *Langmuir* 2005;**21**:10348-54.
12. Ginzburg VV, Balijepalli S. Modeling the thermodynamics of the interaction of nanoparticles with cell membranes. *Nano Lett* 2007;**7**: 3716-22.
13. Bothun GD. Hydrophobic silver nanoparticles trapped in lipid bilayers: size distribution, bilayer phase behavior, and optical properties. *J Nanobiotechnol* 2008;**6**:13.
14. Rasch MR, Rossinyol E, Hueso JL, Goodfellow BW, Arbiol J, Korgel BA. Hydrophobic gold nanoparticle self-assembly with phosphatidylcholine lipid: membrane-loaded and Janus vesicles. *Nano Lett* 2010;**10**: 3733-9.
15. Schulz M, Olubummo A, Binder WH. Beyond the lipid-bilayer: interaction of polymers and nanoparticles with membranes. *Soft Matter* 2012;**8**:4849-64.
16. Nel AE, Madler L, Velegol D, Xia T, Hoek EMV, Somasundaran P, et al. Understanding biophysicochemical interactions at the nano-bio interface. *Nater Mater* 2009;**8**:543-57.

17. Binder WH, Sachsenhofer R, Farnik D, Blaas D. Guiding the location of nanoparticles into vesicular structures: a morphological study. *Phys Chem Chem Phys* 2007;**9**:6435-41.

18. Goodman CM, McCusker CD, Yilmaz T, Rotello VM. Toxicity of gold nanoparticles functionalized with cationic and anionic side chains. *Bioconjug Chem* 2004;**15**:897-900.

19. Arvizo RR, Miranda OR, Thompson MA, Pabelick CM, Bhattacharya R, Robertson JD, et al. Effect of nanoparticle surface charge at the plasma membrane and beyond. *Nano Lett* 2010;**10**:2543-8.

20. Cho EC, Xie J, Wurm PA, Xia Y. Understanding the role of surface charges in cellular adsorption versus internalization by selectively removing gold nanoparticles on the cell surface with a I2/KI Etchant. *Nano Lett* 2009;**9**:1080-4.

21. Shukla R, Bansal V, Chaudhary M, Basu A, Bhonde RR, Sastry M. Biocompatibility of gold nanoparticles and their endocytotic fate inside the cellular compartment: a microscopic overview. *Langmuir* 2005;**21**:10644-54.

22. Fleck CC, Netz RR. Electrostatic colloid-membrane binding. *Europhys Lett* 2004;**67**:314-20.

23. Dreaden EC, Alkilany AM, Huang X, Murphy CJ, El-Sayed MA. The golden age: gold nanoparticles for biomedicine. *Chem Soc Rev* 2012;**41**:2740-79.

24. Dykman LA, Khlebtsov NG. Uptake of engineered gold nanoparticles into mammalian cells. *Chem Rev* 2013;**114**:1258-88.

25. Verma A, Stellacci F. Effect of surface properties on nanoparticle cell interactions. *Small* 2010;**6**:12-21.

26. Pan Y, Neuss S, Leifert A, Fischler M, Wen F, Simon U, et al. Size dependent cytotoxicity of gold nanoparticles. *Small* 2007;**3**:1941-9.

27. Pan Y, Leifert A, Ruau D, Neuss S, Bornemann J, Schmid G, et al. Gold nanoparticles of diameter 1.4 nm trigger necrosis by oxidative stress and mitochondrial damage. *Small* 2009;**5**:2067-76.

28. Turner M, Golovko VB, Vaughan OPH, Abdulkin P, Berenguer-Murcia A, Tikhov MS, et al. Selective oxidation with dioxygen by gold nanoparticle catalysts derived from 55-atom clusters. *Nature* 2008;**454**:981-3.

29. Boon JM, Smith BD. Chemical control of phospholipid distribution across bilayer membranes. *Med Res Rev* 2002;**22**:251-81.

30. Roiter Y, Ornatska M, Rammohan AR, Balakrishnan J, Heine DR, Minko S. Interaction of nanoparticles with lipid membrane. *Nano Lett* 2008;**8**:941-4.

31. Carney RP, Astier Y, Carney TM, Voïtchovsky K, Jacob Silva PH, Stellacci F. Electrical method to quantify nanoparticle interaction with lipid bilayers. *ACS Nano* 2013;**7**:932-42.

32. Chen T, Reinhard BM. Characterizing the lateral friction of nanoparticles on on-chip integrated black lipid membranes. *Small* 2013;**9**:876-84.

33. Reed CA, Roper WR. On the supposed iridium-gold compound $Cl_2(CO)(PPh_3)_2Ir \cdot Au(PPh_3)$. *J Chem Soc A* 1970, http://dx.doi.org/10.1039/J19700000506.

34. Ahrland S, Chatt J, Davies NR, Williams AA. The relative affinities of co-ordinating atoms for silver ion. Part II. Nitrogen, phosphorus, and arsenic. *J Chem Soc* 1958, http://dx.doi.org/10.1039/JR9580000276.

35. Schmid G, Pfeil R, Boese R, Bandermann F, Meyer S, Calis GHM, et al. $Au_{55}[P(C_6H_5)_3]_{12}Cl_6$ — ein goldcluster ungewöhnlicher Größe. *Chem Ber* 1981;**114**:3634-42.

36. Selvakannan PR, Mandal S, Phadtare S, Pasricha R, Sastry M. Capping of gold nanoparticles by the amino acid lysine renders them water-dispersible. *Langmuir* 2003;**19**:3545-9.

37. Olmedo I, Araya E, Sanz F, Medina E, Arbiol J, Toledo P, et al. How changes in the sequence of the peptide CLPFFD-NH₂ can modify the conjugation and stability of gold nanoparticles and their affinity for β-amyloid fibrils. *Bioconjug Chem* 2008;**19**:1154-63.

38. Turkevich J, Stevenson PC, Hillier J. A study of the nucleation and growth processes in the synthesis of colloidal gold. *Discuss Faraday Soc* 1951;**11**:55-75.

39. Leifert A, Pan Y, Kinkeldey A, Schiefer F, Setzler J, Scheel O, et al. Differential hERG ion channel activity of ultrasmall gold nanoparticles. *Proc Natl Acad Sci* 2013;**110**:8004-9.

40. Benz R, Janko K, Boos W, Läuger P. Formation of large, ion-permeable membrane channels by the matrix protein (porin) of *Escherichia coli*. *Biochim Biophys Acta Biomembr* 1978;**511**:305-19.

41. Soares DM, Tenan MA, Gomide AB, Gomes WE. Physical properties of water near a gold surface: a nanorheological analysis. *ChemPhysChem* 2010;**11**:905-11.

42. Schmid G. Developments in transition metal cluster chemistry — the way to large clusters. *Struct Bond* 1985;**62**:51-85.

43. Leifert A, Pan Y, Kinkeldey A, Schiefer F, Setzler J, Scheel O, et al. Differential hERG ion channel activity of ultrasmall gold nanoparticles. *Proc Natl Acad Sci U S A* 2013;**110**:8004-9.

44. Van Lehn RC, Atukorale PU, Carney RP, Yang Y-S, Stellacci F, Irvine DJ, et al. Effect of particle diameter and surface composition on the spontaneous fusion of monolayer-protected gold nanoparticles with lipid bilayers. *Nano Lett* 2013;**13**:4060-7.

45. Agasti SS, You C-C, Arumugam P, Rotello VM. Structural control of the monolayer stability of water-soluble gold nanoparticles. *J Mater Chem* 2008;**18**:70-3.

46. Mei BC, Oh E, Susumu K, Farrell D, Mountziaris TJ, Mattoussi H. Effects of ligand coordination number and surface curvature on the stability of gold nanoparticles in aqueous solutions. *Langmuir* 2009;**25**:10604-11.

47. Zopes D, Stein B, Mathur S, Graf C. Improved stability of "naked" gold nanoparticles enabled by in situ coating with mono and multivalent thiol PEG ligands. *Langmuir* 2013;**29**:11217-26.

48. Weisbecker CS, Merritt MV, Whitesides GM. Molecular self-assembly of aliphatic thiols on gold colloids. *Langmuir* 1996;**12**:3763-72.

49. Isaacs SR, Cutler EC, Park J-S, Lee TR, Shon Y-S. Synthesis of tetraoctylammonium-protected gold nanoparticles with improved stability. *Langmuir* 2005;**21**:5689-92.

50. Hill HD, Millstone JE, Banholzer MJ, Mirkin CA. The role radius of curvature plays in thiolated oligonucleotide loading on gold nanoparticles. *ACS Nano* 2009;**3**:418-24.

51. Cederquist KB, Keating CD. Curvature effects in DNA:Au nanoparticle conjugates. *ACS Nano* 2009;**3**:256-60.

52. Chen H, Langer R, Edwards DA. A film tension theory of phagocytosis. *J Colloid Interface Sci* 1997;**190**:118-33.

53. Pernodet N, Fang X, Sun Y, Bakhtina A, Ramakrishnan A, Sokolov J, et al. Adverse effects of citrate/gold nanoparticles on human dermal fibroblasts. *Small* 2006;**2**:766-73.